

# Influence of Heme Vinyl- and Carboxylate-Protein Contacts on Structure and Redox Properties of Bovine Cytochrome $b_5$

Kang-Bong Lee,<sup>1a</sup> Eunsoon Jun,<sup>1b</sup> Gerd N. La Mar,<sup>\*,1a</sup> Irene N. Rezzano,<sup>1a</sup> Ravindra K. Pandey,<sup>1a</sup> Kevin M. Smith,<sup>1a</sup> F. Ann Walker,<sup>\*,1b,c</sup> and Daniel H. Buttlaire<sup>1b</sup>

Contribution from the Departments of Chemistry, University of California, Davis, California 95616, San Francisco State University, San Francisco, California 94132, and University of Arizona, Tucson, Arizona 85721. Received September 7, 1990

**Abstract:** <sup>1</sup>H NMR spectroscopy and optical spectroelectrochemistry on a thin-layer electrode have been utilized to investigate the influence of heme vinyl- and carboxylate-protein contacts on heme pocket structure and reduction potential of bovine ferricytochrome  $b_5$ . In spite of the diverse modifications of heme vinyls and carboxylates, <sup>1</sup>H NMR results indicate that there are no significant perturbations in the heme orientation and essential electronic structure. This allows us to attribute changes in redox properties to the role of each vinyl- or carboxylate-protein contact in cytochrome  $b_5$ . While pemphothemin (2-H, 4-vinyl) and isopemphothemin (2-vinyl, 4-H) exhibit essentially identical reduction potentials outside the protein in DMF solution, protein reconstituted with pemphothemin shows an  $E^0$  (ca. -8 mV vs SHE) closer to that of native protein (2-vinyl, 4-vinyl; ca. -2 mV), and protein substituted with isopemphothemin exhibits an  $E^0$  (ca. -38 mV) closer to that of deuterohemin (2-H, 4-H; ca. -52 mV). Hence the 4-vinyl group accounts for the dominant electron-withdrawing influence on the porphyrin skeleton of the native protein, with the 2-vinyl group providing a minor effect. These results are consistent with the NMR data which indicate a sterically clamped, largely in-plane (maximal electron withdrawing) 4-vinyl group and a 2-vinyl group that is mobile and largely out of plane (minimal electron withdrawing). The reduction potentials for the cytochrome  $b_5$  complex of 2,4-dimethyldeuterohemin and heptamethyl monoproprionate hemin, with the lone propionate of the latter hemin making the protein link as for the 7-propionate of the native protein, are ca. -83 and ca. -58 mV, respectively. Moreover, the reduction potentials vary insignificantly when the pair of carboxylate side chains are both lengthened or shortened by one carbon. Therefore, the influence on reduction potential for the 7-propionate in the native protein is not substantially larger than that for the 6-propionate, and argues against this uniquely oriented 7-propionate of native cytochrome  $b_5$  providing an important stabilizing interaction for oxidized cytochrome  $b_5$ .

## Introduction

Cytochromes are small heme-containing electron transfer proteins found in a remarkable variety of organisms that exhibit a wide range of reduction potentials even among members with highly conserved prosthetic group and axial ligation.<sup>2,3</sup> Considerable effort has been directed toward understanding the basis of the control of reduction potential by protein structure/environment.<sup>4-18</sup> Factors that modulate heme reduction potentials which have been identified, largely on the basis of work on model complexes and/or selected proteins, are the following: (1) ligation state;<sup>5,6</sup> (2) environment (heme pocket) hydrophobicity;<sup>7-10</sup> (3) electrostatic interactions;<sup>11,12</sup> (4) axial His imidazole orientation;<sup>13</sup>

(5) hydrogen bonding by the axial His;<sup>14,15</sup> and (6) orientation of heme substituents.<sup>16-18</sup> A particularly effective approach to identifying controlling influences on reduction potential is to monitor the potential upon subjecting a specific protein to systematic perturbations of the proposed structural determinants of the potential in as specific and unique a manner as possible. Such perturbations can be effected via either site-directed mutagenesis of the polypeptide chain<sup>19,20</sup> or, for  $b$ -type cytochromes, chemical modification of the prosthetic group.<sup>12,17</sup> While both methods should yield important information, the latter approach has the advantage of allowing the introduction of a wider variety of systematic perturbations.

We focus in this report on the solubilized fragment of bovine microsomal cytochrome  $b_5$ , a small polypeptide of 93 amino acids possessing a single bound protohemin group<sup>21</sup> (1B in Figure 1), whose high-resolution X-ray crystal structure has been solved in both oxidation states.<sup>18,22,23</sup> This fragment retains the functional properties of the membrane bound holoprotein that is involved in fatty acid desaturation<sup>24-26</sup> and is essentially identical with the erythrocyte hemoglobin reductase electron mediator.<sup>27</sup> The orientation of one propionate (at position g in A of Figure 1) toward the iron was proposed<sup>18</sup> to serve as a charge-stabilizing mechanism for the oxidized protein and has been used to rationalize the low reduction potential. Measurements of the reduction potential of the native protein, as well as that reconstituted

(1) (a) University of California, Davis. (b) San Francisco State University. (c) Present address: University of Arizona.

(2) Meyer, T. E.; Cusanovich, M. A. *Biochim. Biophys. Acta* **1989**, *975*, 1-28.

(3) Bartsch, R. G. In *The Photosynthetic Bacteria*; Clayton, R. K., Sistrom, W. R., Eds.; Plenum Press: New York, 1978; pp 249-275.

(4) Cusanovich, M. A.; Meyer, T. E.; Tollin, G. In *Advances in Inorganic Biochemistry*; Eichhorn, G. L., Marzilli, L. G., Eds.; Elsevier: New York, 1988; pp 37-91.

(5) Mashiko, T.; Reed, C. A.; Haller, K. J.; Kastner, M. E.; Scheidt, W. R. *J. Am. Chem. Soc.* **1981**, *103*, 5758-5767.

(6) Moore, G. R.; Williams, R. J. P. *FEBS Lett.* **1977**, *79*, 229-232.

(7) Pettigrew, G. W.; Meyer, T. E.; Bartsch, R. G.; Kamen, M. D. *Biochim. Biophys. Acta* **1975**, *430*, 197-208.

(8) Pettigrew, G. W.; Bartsch, R. G.; Meyer, T. E.; Kamen, M. D. *Biochim. Biophys. Acta* **1978**, *503*, 509-523.

(9) Moore, G. R.; Harris, D. E.; Leitch, F. A.; Pettigrew, G. W. *Biochim. Biophys. Acta* **1984**, *764*, 331-342.

(10) Kassner, R. J. *Proc. Natl. Acad. Sci. U.S.A.* **1970**, *69*, 2263-2267.

(11) Moore, G. R. *FEBS Lett.* **1983**, *161*, 171-175.

(12) Reid, L. S.; Mauk, M. R.; Mauk, A. G. *J. Am. Chem. Soc.* **1984**, *106*, 2182-2185.

(13) Geiger, D. K.; Lee, Y. J.; Scheidt, W. R. *J. Am. Chem. Soc.* **1984**, *106*, 6339-6343.

(14) Valentine, J. S.; Sheridan, R. P.; Allen, L. C.; Kahn, P. C. *Proc. Natl. Acad. Sci. U.S.A.* **1979**, *76*, 1009-1013.

(15) Doeff, M. M.; Sweigart, D. A.; O'Brien, P. *Inorg. Chem.* **1983**, *22*, 851-852.

(16) Brunori, M.; Saggese, U.; Rotilio, G. C.; Antonini, E.; Wyman, J. *Biochemistry* **1971**, *10*, 1604-1609.

(17) Reid, L. S.; Lim, A. R.; Mauk, A. G. *J. Am. Chem. Soc.* **1986**, *108*, 8197-8201.

(18) Argos, P.; Mathews, F. S. *J. Biol. Chem.* **1975**, *250*, 747-751.

(19) von Bodman, S. B.; Schuler, M. A.; Jollie, D. R.; Sligar, S. G. *Proc. Natl. Acad. Sci. U.S.A.* **1986**, *83*, 9443-9447.

(20) Funk, W. D.; Lo, T. P.; Mauk, M. R.; Brayer, G. D.; MacGillivray, T. A.; Mauk, A. G. *Biochemistry* **1990**, *29*, 5500-5508.

(21) Mathews, F. S.; Czerwinski, E. W.; Argos, P. In *The Porphyrins*; Dolphin, D., Ed.; Academic Press: New York, 1979; Vol. 7, pp 107-147.

(22) Mathews, F. S.; Argos, P.; Levine, M. *Cold Spring Harbor Symp. Quant. Biol.* **1971**, *36*, 387-395.

(23) Mathews, F. S. *Biochim. Biophys. Acta* **1980**, *622*, 375-379.

(24) Strittmatter, P.; Spatz, L.; Concoran, D.; Rogers, M. T.; Setlow, B.; Redline, R. *Proc. Natl. Acad. Sci. U.S.A.* **1974**, *71*, 4565-4569.

(25) Tamburini, P. P.; Scheukman, J. B. *Arch. Biochem. Biophys.* **1986**, *245*, 5512-5522.

(26) Ozols, J. *J. Biol. Chem.* **1972**, *247*, 2242-2245.

(27) Hultquist, D. E.; Sannes, L. G.; Juckett, D. A. *Curr. Top. Cell. Reg.* **1984**, *24*, 287-300.

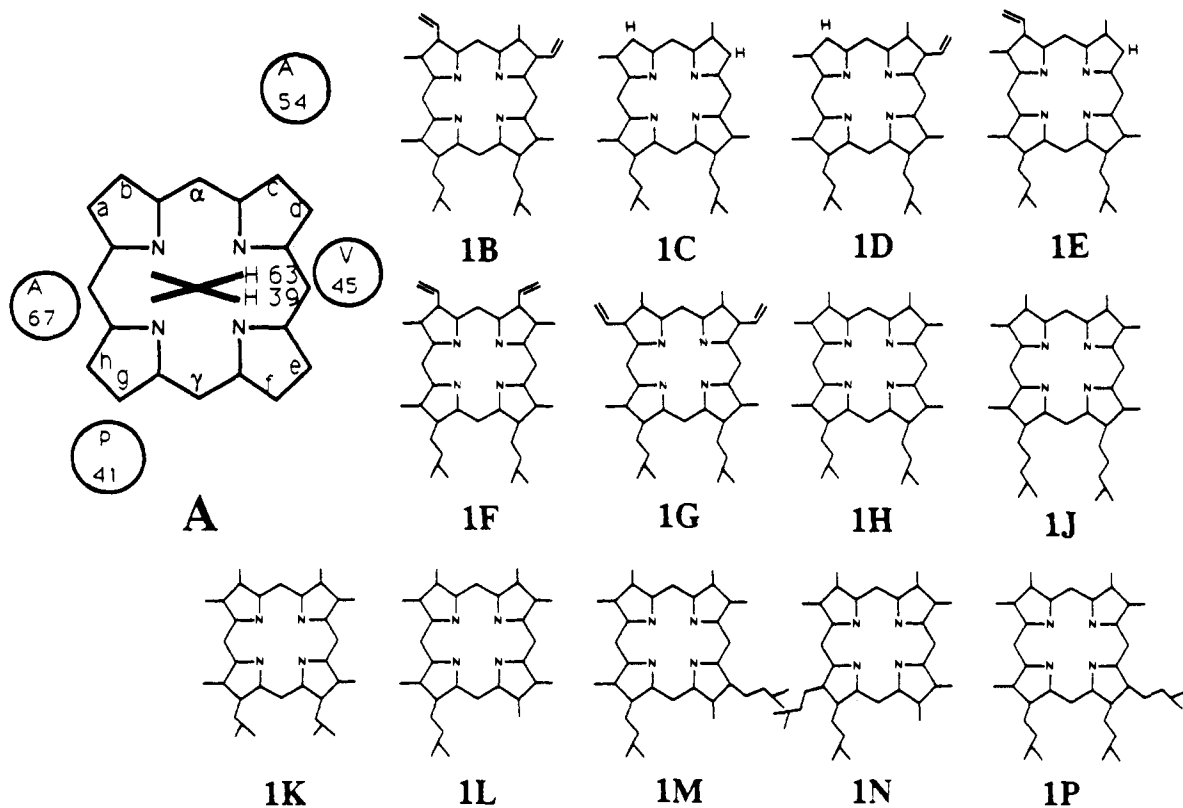


**Figure 1.** The porphyrin skeleton in the protein matrix as elucidated in the crystal structure of bovine cytochrome *b*<sub>5</sub>; all substituents are deleted. Instead we identify the eight nonequivalent pyrrole positions by letters a → h which are occupied by the substituents 1 → 8, respectively, in the major form detected in the corrected crystal structure. We use this labeling scheme to identify where methyls, vinyls, single protons, and propionates are located in the protein matrix, and this, in turn, establishes the orientation of a particular hemin in the pocket (1B → 1P). The particular orientation of each of the hemins with respect to some specified amino acid residues was selected to correspond to the equilibrium orientation, where stable reconstituted complexes result, established by <sup>1</sup>H NMR spectroscopy, viewing the hemes from the same perspective.

with deuterohemin (1C in Figure 1) and native hemin esterified at both propionates, were interpreted to support the electrostatic influence of the protein-bound propionate.<sup>12,20,28</sup> It was also proposed<sup>17,29</sup> that the reduction potential is modulated by the degree of coplanarity with the heme (and hence electron withdrawing influence) of the vinyl groups.

It would be desirable in addressing the role of propionates and/or vinyl groups in modulating electronic structure and reduction potential to introduce modifications one at a time to assess the roles of the individual rather than a pair of heme substituents. We present herein a study of the solution structure and reduction potential of bovine ferricytochrome *b*<sub>5</sub> reconstituted with a wide variety of modified hemins designed to introduce as selectively as possible perturbations on the carboxylate interaction without modifying the remaining heme-protein interaction, as well as on the heme vinyl-protein interaction without altering the heme carboxylate-protein interaction. Prior to measuring the reduction potential, *E*<sup>0</sup>, however, it is essential to know if the reconstituted complex is homogeneous and to uniquely identify the orientation of the hemin in the cavity. This is important because native cytochromes *b*<sub>5</sub> exhibits extensive and variable heme orientational disorder<sup>30,31</sup> about the heme α,γ-meso axis in Figure 1A, and the heme orientation itself is known<sup>32</sup> to have a small but detectable effect on *E*<sup>0</sup>.

A wide variety of hemins has been synthesized in addition to native hemin, 1B, and deuterohemin, 1C, and include replacements

of the vinyls, one at a time, with hydrogen<sup>33</sup> (hemins 1D and 1E), or interchanging methyls and vinyls to yield symmetric hemins<sup>34</sup> 1F and 1G. We had discovered previously that modification of the carboxylate side chain<sup>35</sup> leads to competing influences on heme orientation from the vinyl and carboxylate side chains.<sup>36</sup> Hence, we pursue the investigation of carboxylate side chain number, length, and position on a series of hemins that possess only methyl and carboxylate side chains; i.e. the orienting influence of the asymmetrically placed vinyls is abolished. Such hemins can be considered members of the isomeric complexes, (methyl)<sub>n</sub>(propionate)<sub>8-n</sub>porphine-iron(III), for which hemin 1H provides the symmetric analogue to native hemin, and 1J and 1K represent the lengthening (butyrates) and shortening (acetates) of the two carboxylate chains for the symmetric skeleton. The (methyl)<sub>n</sub>(propionate)<sub>8-n</sub>porphine-iron(III) skeleton also conveniently provides a monopropionate isomer, hemin 1L, which, upon comparison to 1H, will allow the assessment of the influence of removing a single propionate. Moreover, this skeleton also allows for altering the positions on the hemin for the two propionates (hemins 1M and 1N) or addition of a third propionate, 1P. The <sup>1</sup>H NMR spectra of all of the above hemins 1B through 1H have been reported<sup>37</sup> for both rat and bovine reconstituted ferricytochrome *b*<sub>5</sub>, and those of hemin 1L-1P have been described<sup>36</sup> solely for the rat ferricytochrome *b*<sub>5</sub>; NMR spectra of ferricytochrome *b*<sub>5</sub> complexes of symmetric hemin 1J and 1K have not been reported previously. All <sup>1</sup>H NMR characterized ferricytochrome *b*<sub>5</sub> complexes yielded a predominantly or wholly homogeneous solution for which the orientation of all heme sub-

(28) Reid, L. S.; Taniguchi, V. T.; Gray, H. B.; Mauk, A. G. *J. Am. Chem. Soc.* **1982**, *104*, 7516-7519.

(29) Balke, V. L.; Walker, F. A.; West, J. T. *J. Am. Chem. Soc.* **1985**, *107*, 1226-1233.

(30) La Mar, G. N.; Burns, P. D.; Jackson, J. T.; Smith, K. M.; Langry, K. C.; Strittmatter, P. *J. Biol. Chem.* **1981**, *256*, 6075-6079.

(31) McLachlan, S. J.; La Mar, G. N.; Burns, P. D.; Smith, K. M.; Langry, K. C. *Biochim. Biophys. Acta* **1986**, *874*, 274-284.

(32) Walker, F. A.; Emrick, D.; Rivera, J. E.; Hanquet, B. J.; Buttlar, D. H. *J. Am. Chem. Soc.* **1988**, *110*, 6234-6240.

(33) Johnson, A. W. *The Porphyrins*; Dolphin, D., Ed.; Academic Press: New York, 1979; Vol. 1, pp 235-264.

(34) Smith, K. M.; Parish, D. W.; Inouye, W. S. *J. Org. Chem.* **1986**, *51*, 666-671.

(35) Smith, K. M.; Craig, G. W. *J. Org. Chem.* **1983**, *48*, 4302-4306.

(36) Lee, K.-B.; La Mar, G. N.; Pandey, R. K.; Rezzano, I. N.; Mansfield, K. E.; Smith, K. M. *Biochemistry* **1991**, *30*, 1878-1887.

stituents within the protein matrix (see Figure 1A) were clearly identified<sup>37-40</sup> by the nuclear Overhauser effect.<sup>41</sup>

### Experimental Section

**Preparation of Samples.** Trypsin-solubilized beef cytochrome *b*<sub>5</sub> was isolated from fresh calf liver and purified to an optical purity index (*A*<sub>412</sub>/*A*<sub>280</sub>) of ~5.8 as described earlier.<sup>42,43</sup> Apoprotein was prepared according to the reported procedure.<sup>44</sup> The chemically modified hemins used in this study were synthesized as described previously.<sup>33-35</sup> Apoprotein was reconstituted by adding a stoichiometric amount of hemin dissolved in 0.1 M NaO<sup>2</sup>H to a 0.4-mL solution of 1–3 mM apoprotein in 0.1 M deuterated phosphate buffer. Aqueous pyridine (50%) was used to dissolve hemins **1H** and **1K–1P**, since these were insufficiently soluble in alkaline aqueous medium. Heme incorporation was monitored optically (Hewlett-Packard 8540A UV-visible spectrophotometer) with use of 1 cm light path quartz cells referenced to water. The titrations yielded clean 1:1 break points and the characteristic ~10 nm red shift of the Soret band upon incorporation into the heme pocket. The holoproteins reconstituted with chemically modified hemins were immediately passed through a Sephadex G-75 column and lyophilized. The sample was finally concentrated to ~1 mM in <sup>2</sup>H<sub>2</sub>O. The pH of all samples was controlled by adding <sup>2</sup>HCl or NaO<sup>2</sup>H as necessary; the pH values were uncorrected for the isotope effect.

**<sup>1</sup>H NMR Measurements.** <sup>1</sup>H NMR spectra were recorded at 25 °C on Nicolet NT-500 spectrometers operating in the quadrature mode at 500 MHz. Data were collected by using double precision on 16384 data points over an approximately ±15-kHz bandwidth at 500 MHz. Typical spectra consisted of ~3000 transients with a repetition rate of 1.2 s<sup>-1</sup>. Chemical shifts for all spectra are referenced to 2,2-dimethyl-2-silapentane-5-sulfonate, DSS, through the residual water resonance. The steady-state nuclear Overhauser effect,<sup>41</sup> NOE,  $\eta_{ij}$ , is defined as

$$\eta_{ij} = \frac{(I_j - I_j^0)}{I_j^0} = \sigma_{ij} T_{1j} \quad (1)$$

where  $I_j$  and  $I_j^0$  are intensities for the signal from the detected proton  $H_j$  with and without saturating the resonance of the spin  $H_i$ ,  $T_{1j}$  is the selective spin-lattice relaxation time of  $H_j$ , and  $\sigma_{ij}$  is the cross-relaxation rate between  $H_i$  and  $H_j$ . The NOE spectra were recorded according to

$$(A[t_1 - t_{\text{on}} - P - \text{Acq}]_n B[t_1 - t_{\text{off}} - P - \text{Acq}]_n)_{nm} \quad (2)$$

where *A* and *B* designate two different data files,  $t_1$  is a preparation time to allow the relaxation of the resonance (500 ms),  $t_{\text{on}}$  is the time during which the resonance is kept saturated (200 ms), and  $t_{\text{off}}$  is an equal time (200 ms) during which the decoupler is set off-resonance. *P* is the observed 90° pulse. *n* was set to 96, and the total number of scans in each file (*nm*) was ~3 × 10<sup>3</sup>. The NOE difference spectra were obtained by subtracting *B* from *A*.

**Spectroelectrochemistry.** The anaerobic spectrochemical thin cell and the mechanical system for the spectroelectrochemical titration were designed as described previously.<sup>32,45-47</sup> A 3.0-mL sample of the protein solution (60 μM) containing 0.2 mM Ru(NH<sub>3</sub>)<sub>6</sub>Cl<sub>3</sub>, 0.2 mM K<sub>3</sub>Fe(CN)<sub>6</sub>, 1 mM methyl viologen, and 0.13 M phosphate buffer (pH 7.0) was prepared, degassed, and introduced into the cell, as before.<sup>32</sup> The reference used was a Bioanalytical systems Ag/AgCl electrode ( $E^0 = -27$  mV vs SCE). Spectra were recorded on a Hewlett-Packard 8451A diode array spectrophotometer and the potential was applied by utilizing a PAR Model 173 potentiostat. The solution was pre-electrolyzed as before, first at -400 mV, then at 0 mV, and again at -400 mV vs Ag/AgCl for 20 min each.<sup>32</sup> After this redox cycle, the potential was increased and decreased in a stepwise fashion through the potential range -355 to -155 mV vs Ag/AgCl. The absorbance at the Soret  $\lambda_{\text{max}}$  for each modified

**Table I.** Chemical Shifts for Resolved Hemin and Selected Amino Acid Residues for Bovine Ferricytochrome *b*<sub>5</sub> Reconstituted with Modified Hemins<sup>a</sup>

peak symbol/assign <sup>b</sup>	hemins <sup>c</sup>					
	1H	1J	1K	1L	1M	1N
M <sub>a</sub>	15.00	11.39	14.07	14.45	15.74	15.22
M <sub>b</sub>	31.67	28.95	29.25	31.13	31.24	26.03
M <sub>c</sub>	14.57	19.10	15.41	15.24	14.87	16.14
M <sub>d</sub>	1.20	4.60	<i>d</i>	<i>d</i>	<i>d</i>	1.50
M <sub>e</sub> (H <sub>e</sub> )	21.58	16.88	21.78	22.06	12.78	20.32
H <sub>f</sub> (M <sub>f</sub> )	15.73	14.53	16.18	34.30	34.15	28.66
H <sub>g</sub>	18.95	18.93	20.63	18.36	18.17	16.56
M <sub>h</sub> (H <sub>h</sub> )	2.01	6.75	<i>d</i>	<i>d</i>	<i>d</i>	0.21
H <sub>39</sub> /His 39 C <sub>β</sub> H	16.09	16.02	17.32	16.16	16.54	14.79
L <sub>46</sub> /Leu 46 C <sub>β</sub> H <sub>3</sub>	-3.16	-2.03	-2.26	-3.11	-2.99	-2.33
H <sub>39</sub> '/His 39 ring CH	-12.3	-11.2	-11.9	-13.2	-13.4	-13.1

<sup>a</sup> In ppm from DSS, in <sup>2</sup>H<sub>2</sub>O solution at 25 °C. <sup>b</sup> Hemin substituent, M<sub>i</sub>, H<sub>i</sub>, peaks labeled according to position occupied in the protein matrix as defined in A of Figure 1. <sup>c</sup> The hemins have their structure depicted in Figure 1. <sup>d</sup> Not assigned (under diamagnetic envelope).

cytochrome *b*<sub>5</sub> was monitored over a period of 10–15 min at each applied potential until a stable reading was obtained, after which time the spectrum was recorded over the wavelength range 300–800 nm. Tight isobestic points were observed during a run, indicating no measurable denaturation of the protein during the electrochemical titration.

Spectroelectrochemical titrations of pempto- and isopemtohemins were carried out in dimethylformamide, DMF (Fisher Spectraanalyzed, used as received), utilizing 0.1 M tetrabutylammonium perchlorate, TBAP (Southwestern Analytical, purified as before<sup>48</sup>), as electrolyte and 0.1 M *N*-methylimidazole, NMeIm (Aldrich, distilled), as the axial ligand. The cells utilized for these titrations were fashioned from Delrin according to the design of the Lucite cells used for titration of protein solutions in this study and previously.<sup>32</sup> Porphyrin concentrations were the following: pemptohemin Cl, 0.01 mM; isopemtohemins Cl, 0.006 mM. No mediators were utilized for these hemin titrations in DMF. The titrations were carried out as described above except for the potential ranges utilized: pre-oxidation was carried out at +100 mV, pre-reduction at -350 mV, and the titration between -225 and -60 mV vs Ag/AgCl. Because the ferrous forms appeared to adsorb on the electrodes, the time between adjusting the potential and recording the spectrum was 3 min for each titration step.

### Results

**Solution Structure. (a) Orientation of Asymmetric Hemins.** The <sup>1</sup>H NMR spectra of native bovine ferricytochrome *b*<sub>5</sub> and the reconstituted products with deuterohemin (**1C**), pemptohemin (**1D**), and isopemtohemins (**1E**) have been reported and assigned previously.<sup>30,37,49</sup> The proteins of hemin **1C** and **1E** are essentially homogeneous (minor component <2%), while that of hemin **1D** exhibits 20% minor component.<sup>37</sup> The dominant orientation in each case has the vinyl and H at the same position as the native vinyls (positions *b* and *d* in Figure 1A). The <sup>1</sup>H NMR spectra of the bovine ferricytochrome *b*<sub>5</sub> complexes reconstituted with the asymmetric (methyl)<sub>*n*</sub>(propionate)<sub>*g-h*</sub>porphine-iron(III) isomers, hemins **1L**, **1M**, and **1N** (Figure 2), as well as that for hemin **1P** (not shown), are essentially the same as those for the analogous rat protein complexes reported previously<sup>36</sup> and hence assignments result simply by analogy. The complex of hemin **1N** exhibits somewhat larger shifts than in the rat protein; selected 1D NOEs (not shown; see Supplementary Material) for the bovine complex provide the assignments given in Figure 2C and confirm that the unique orientation is the same as that found for the rat ferricytochrome *b*<sub>5</sub> complex of the same hemin.<sup>36,37</sup> Hence, the propionates are at position *g* for hemin **1L**, at positions *g* and *e* for hemin **1M**, and at positions *g* and *h* for hemin **1N**. The three propionates for hemin **1P** were shown to reside at positions *e*, *f*, and *g* in rat ferricytochrome *b*<sub>5</sub>, and the same orientation is assumed for the bovine protein complex of this hemin. The chemical shifts for the bovine protein complexes are included in Table I.

(48) Walker, F. A.; Barry, J. A.; Balke, V. L.; McDermott, G. A.; Wu, M. Z.; Linde, P. F. *Adv. Chem. Ser.* **1982**, *201*, 377-416.

(49) Keller, R. M.; Groudinsky, O.; Wüthrich, K. *Biochim. Biophys. Acta* **1976**, *427*, 497-511.

(37) Lee, K.-B.; La Mar, G. N.; Kehres, L. A.; Fujinari, E. M.; Smith, K. M.; Pochapsky, T.; Sligar, S. G. *Biochemistry* **1990**, *29*, 9623-9631.

(38) Keller, R. M.; Wüthrich, K. *Biochim. Biophys. Acta* **1980**, *521*, 204-217.

(39) McLachlan, S. J.; La Mar, G. N.; Sletten, E. J. *Am. Chem. Soc.* **1986**, *108*, 1285-1291.

(40) McLachlan, S. J.; La Mar, G. N.; Lee, K.-B. *Biochim. Biophys. Acta* **1988**, *957*, 430-445.

(41) Neuhaus, D.; Williamson, M. *The Nuclear Overhauser Effect*; VCH Publishers: New York, 1989.

(42) Reid, L. S.; Mauk, A. G. *J. Am. Chem. Soc.* **1982**, *104*, 841-845.

(43) McLachlan, S. J. Ph.D. Thesis University of California, Davis, 1988.

(44) Teale, F. W. J. *Biochim. Biophys. Acta* **1959**, *35*, 543.

(45) Bowen, E. F.; Hawkrige, F. M. *J. Electroanal. Chem. Interfacial Electrochem.* **1981**, *125*, 367-386.

(46) Norris, B. J.; Meckstroth, M. L.; Heineman, W. R. *Anal. Chem.* **1976**, *48*, 630-632.

(47) Balfe, C. A. Ph.D. Thesis University of California, Berkeley, 1984.

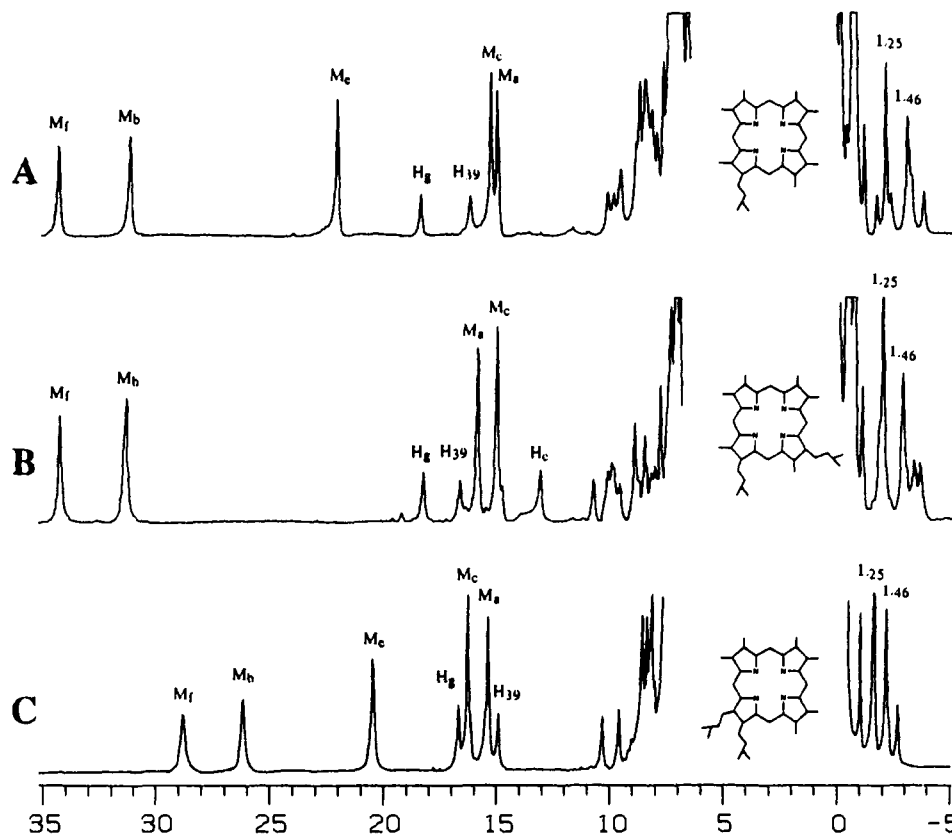


**Figure 2.** The hyperfine-shifted region of the 500-MHz  $^1\text{H}$  NMR spectra of bovine ferricytochrome *b*<sub>5</sub> reconstituted with hemins **1L**, **1M**, and **1N** at equilibrium state in  $^2\text{H}_2\text{O}$  solution, 25 °C: (A) protein reconstituted with hemin **1L** at pH 7.30; (B) protein reconstituted with hemin **1M** at pH 7.30; (C) protein reconstituted with hemin **1N** at pH 7.24.

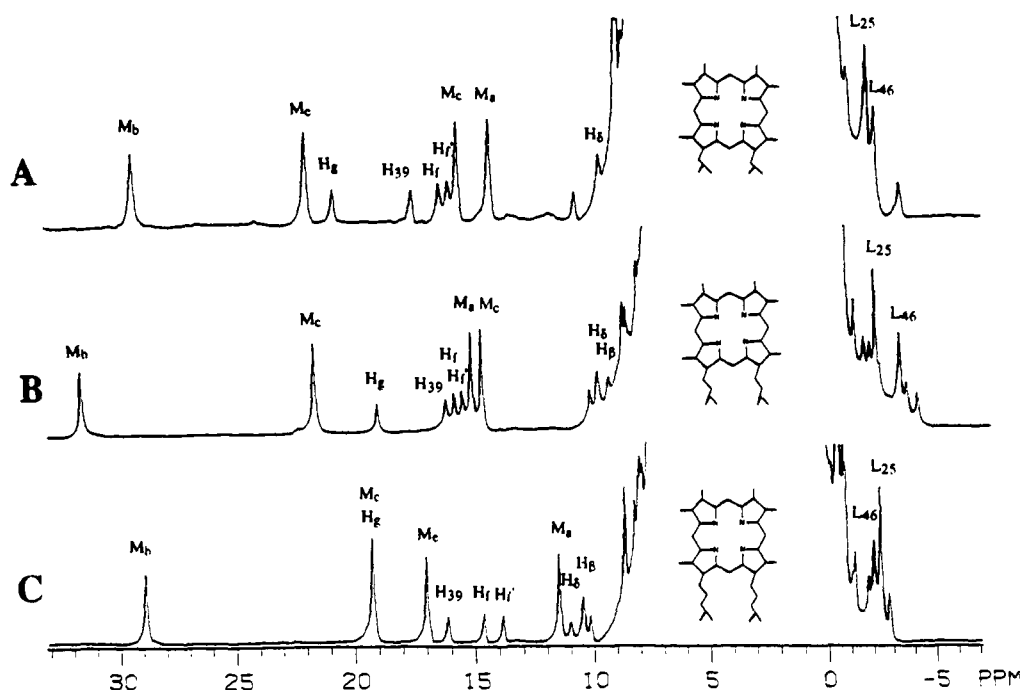


**Figure 3.** The hyperfine-shifted region of the 500-MHz  $^1\text{H}$  NMR spectra of equilibrated bovine ferricytochrome *b*<sub>5</sub> substituted with hemins **1K**, **1H**, and **1J** in  $^2\text{H}_2\text{O}$  solution, 25 °C: (A) protein reconstituted with hemin **1K** at pH 7.24; (B) protein reconstituted with hemin **1H** at pH 7.59; (C) protein reconstituted with hemin **1J** at pH 7.36.

(b) **Symmetric Hemins.** The  $^1\text{H}$  NMR trace of the 2,4-dimethyldeuteriohemine complex of bovine ferricytochrome *b*<sub>5</sub>, **1H**, illustrated in Figure 3B, has been assigned previously.<sup>37</sup> The traces of bovine ferricytochrome *b*<sub>5</sub> reconstituted with the analogous hemin with the elongated butyrate (hemin **1J**) and abbreviated acetate (hemin **1K**) side chains are shown in Figure 3, C and A, respectively. The detailed assignments given in Figure 3 were

obtained by 1D NOEs<sup>36</sup> (not shown) are very similar to those of the protein complex of hemin **1H**. The variable carboxylate chain lengths result in relatively small perturbations of the contact shift pattern for these three necessarily homogeneous protein complexes. The chemical shift data are presented in Table I.

(c) **Orientation of Vinyls.** Detailed analysis<sup>40</sup> of the pattern of NOEs from the individual vinyl protons to the adjacent methyls

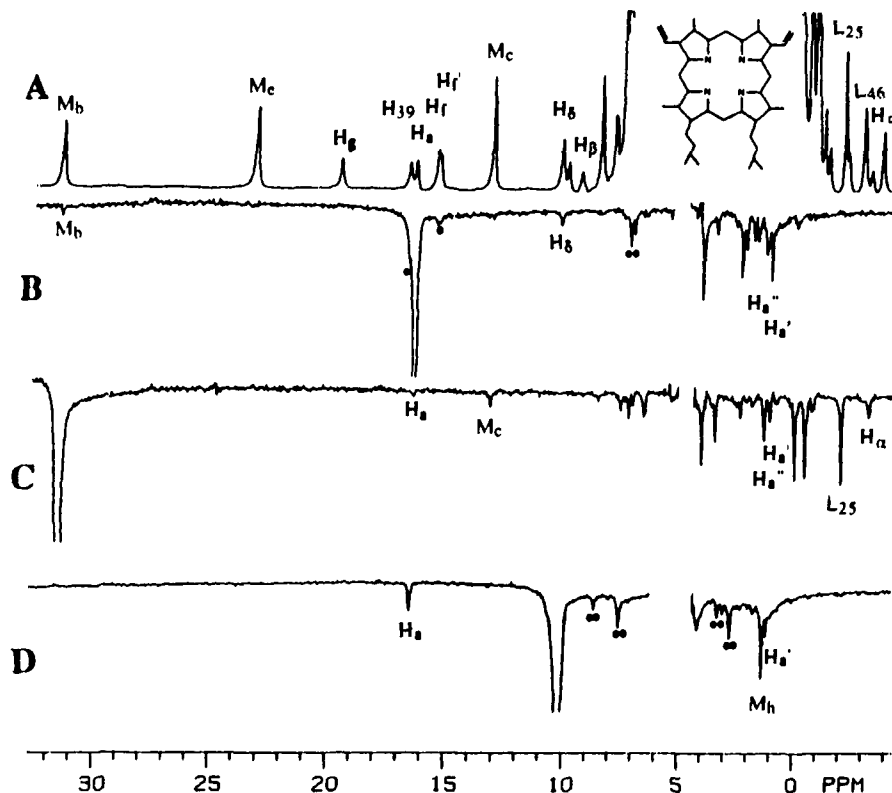


**Figure 4.** Steady-state NOE difference spectra of ferricytochrome  $b_5$  reconstituted with protohemin XIII in  $^2\text{H}_2\text{O}$  solution, 25 °C and pH 7.62: (A) reference spectrum; (B) following saturation of peak  $H_\alpha(H_\alpha)$ , note NOEs to  $M_b$ ,  $H_b$ ,  $H_\alpha'$ , and  $H_\alpha''$ ; (C) following saturation of peak  $M_b$  (2- $\text{CH}_3$ ), note NOEs to  $H_\alpha$ ,  $M_c$ ,  $H_\alpha'$ ,  $H_\alpha''$ ,  $L_{25}$ , and  $H_\alpha$  ( $\alpha$ -meso); (D) following saturation of  $H_\alpha$ , note NOEs to  $H_\alpha$  (1- $H_\alpha$ ),  $M_b$  (8- $\text{CH}_3$ ), and  $H_\alpha'$  (1- $H_{\beta c}$ ); difference peaks due to off-resonance saturation (power spillage) are marked as filled circles and NOE peaks due to off-resonance saturation are marked as filled double circles.

and meso-H for native bovine ferricytochrome  $b_5$  had shown close spatial proximity of both  $\alpha$ -meso-H and 1- $\text{CH}_3$  to both  $H_\alpha$  and  $H_{\beta 1}$  of the 2-vinyl group located in position b in Figure 1A. In contrast, the NOE pattern involving the 4-vinyl group at position d in Figure 1A revealed close proximity solely between 3- $\text{CH}_3$  and 4- $H_{\beta 1}$  and  $\beta$ -meso-H and 4- $H_\alpha$ .

The 500-MHz  $^1\text{H}$  NMR trace of bovine ferricytochrome  $b_5$  reconstituted with symmetric protohemin XIII (hemin 1G) is reproduced in Figure 4A, together with the reported assignments. Irradiation of a single proton  $H_\alpha$  generates NOEs to  $M_b$  and  $H_b$  ( $\delta$ -meso-H) which confirms that peak  $H_\alpha$  is from 1- $H_\alpha$  of the vinyl group at position a. Saturation of the methyl at position b,  $M_b$ , yields NOEs to both  $H_\alpha$  ( $H_\alpha$ ) and  $H_{\beta s}$  ( $H_\alpha'$ ,  $H_\alpha''$ ) with magnitudes to each vinyl position comparable to those observed previously<sup>40</sup> for the 1- $\text{CH}_3$  to 2-vinyl group in the native protein. Similarly, saturation of the  $\delta$ -meso-H peak,  $H_b$ , yields NOEs to both 2-vinyl  $H_\alpha$  ( $H_\alpha$ ),  $H_{\beta c}$  ( $H_\alpha'$ ), and  $M_h$  as shown in Figure 4D. Hence, the orientation and mobility of the 2-vinyl group at position b of the native protein are very similar to those of the 1-vinyl group at position a in the protohemin 1G) complex of bovine ferricytochrome  $b_5$ .

The 500-MHz  $^1\text{H}$  NMR trace of the protohemin III (hemin 1F) complex of bovine ferricytochrome  $b_5$  and the previous methyl assignments<sup>37</sup> are reproduced in Figure 5A; it is noted that the shifts (as well as NOEs; not shown) of the invariant 2-vinyl group at position b are unchanged from those of the native protein. Characteristic multiplet structure (not shown) identifies  $H_c'$ ,  $H_c''$  as the c position or 3-vinyl  $H_{\beta 1}$  and  $H_{\beta c}$ , respectively. Saturation of  $H_c'$  exhibits an NOE to the methyl at position d,  $M_d$ , as well as the expected NOE to the vinyl  $H_\alpha$  peak  $H_c$  (Figure 5B). Conversely, irradiation of  $\alpha$ -meso-H peak  $H_\alpha$  (Figure 5C) exhibits a large NOE to  $H_c$  (3-vinyl  $H_\alpha$ ), but not to the  $H_\beta$  peaks,  $H_c'$ ,  $H_c''$ . Moreover, the  $\alpha$ -meso-H NOE to the 3- or c-position vinyl  $H_\alpha$  ( $H_c$ ) is 4–5 times larger than that to the 2- or b-position vinyl  $H_\alpha$  ( $H_\alpha$ ). Hence the NOE pattern for the c-vinyl and d-methyl in the protohemin III (hemin 1F) complex is the same as for the c-methyl and d-vinyl of the native protein,<sup>40</sup> which dictates that

the orientations of the vinyl groups relative to the heme for positions c and d are similar, but distinct, from those at positions a or b.

**Reduction Potentials.** The electronic absorption spectra of both oxidation states of cytochrome  $b_5$  were similar to those reported earlier.<sup>50</sup> The Soret band maxima (nm) of the oxidized derivatives are as follows: 404 (hemins 1C and 1L), 406 (hemins 1H, 1J, 1K, 1M, and 1N), 408 (hemins 1D and 1E), 412 (hemins 1G and 1P), and 414 (hemins 1B and 1F). The difference ( $A_{\text{red}} - A_{\text{ox}}$ ) spectra for cytochrome  $b_5$  reconstituted with hemin 1F are shown in Figure 6, which depicts a typical family of spectra obtained during a spectroelectrochemical titration experiment. The data of Figure 6 were analyzed according to the Nernst equation (eq 3), utilizing Beer's law to calculate the concentration ratio of oxidized to reduced protein for each of the difference spectra.<sup>51</sup>

$$E = E^0 + (RT/nF) \ln \frac{[\text{ferricytochrome } b_5]}{[\text{ferrocyanochrome } b_5]} \quad (3)$$

The resulting Nernst plot is shown in the inset of Figure 6. The calculated reduction potentials were converted to the standard hydrogen electrode at 28 °C by adding 209 mV.<sup>51</sup> The average midpoint reduction potentials obtained from Nernst plots of various modified heme-substituted cytochrome  $b_5$  are tabulated in Table II. The reduction potential of bovine ferricytochrome  $b_5$  has been shown to be pH dependent,<sup>28</sup> with apparent  $\text{pK} \sim 5.9$ . However, this  $\text{pK}$  is unaffected by diesterification of the hemin<sup>12</sup> and hence is unrelated to the state of the propionates. Our determination of reduction potentials was restricted to pH  $\sim 7.0$ , where the small influence of this protein-centered  $\text{pK}$  is negligible. Hence, the observed differences in  $E^0$  must reflect primarily electronic differences due to the heme peripheral perturbations.

The purpose of the spectroelectrochemical measurements on model hemins in DMF was to determine whether pempto- and isopemtohemins ( $\text{NMeIm}$ )<sub>2</sub><sup>+</sup> had the same or different reduction

(50) Ozols, J.; Strittmatter, P. *J. Biol. Chem.* **1964**, *239*, 1018–1023.  
(51) Dulton, P. L. *Methods Enzymol.* **1978**, *54*, 411–435.

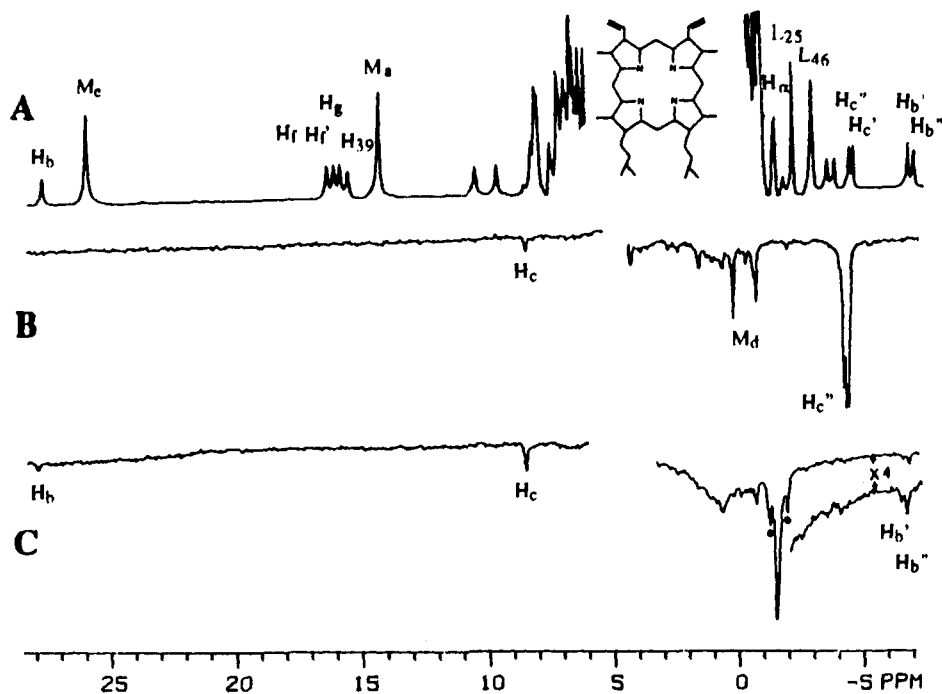


**Figure 5.** Steady-state NOE difference spectra of ferricytochrome *b*<sub>5</sub> reconstituted with protohemin III, 1F, in <sup>2</sup>H<sub>2</sub>O solution, 25 °C and pH 7.70: (A) reference spectrum; (B) following saturation of peak H<sub>c</sub>' (3-H<sub>βc</sub>), note NOEs to H<sub>c</sub> and M<sub>d</sub>; (C) following saturation of peak, H<sub>a</sub> (α-meso); note NOEs to H<sub>b</sub>, H<sub>b</sub>', H<sub>b</sub>'', and M<sub>c</sub>, and no NOEs to H<sub>c</sub>' and H<sub>c</sub>''; difference peaks due to off-resonance saturation (power spillage) are marked as filled circles.

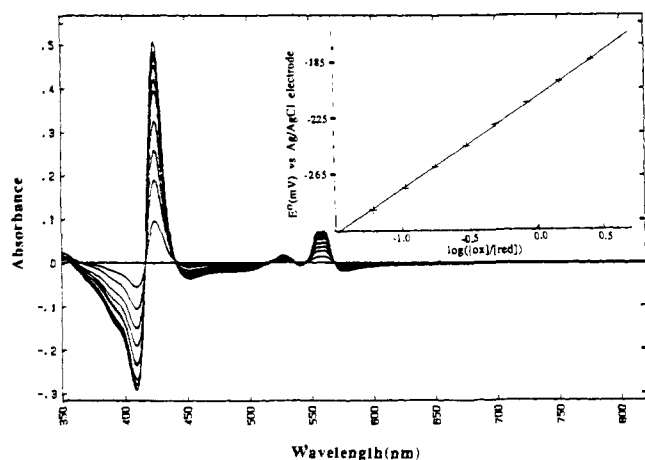


**Figure 6.** Representative optical difference spectra obtained from spectroelectrochemical titration of cytochrome *b*<sub>5</sub> reconstituted with hemin 1F in the presence of the three mediators as discussed in the text. The extremes represent the fully reduced minus fully oxidized spectra. Inset: the Nernst plot of the same data; slope = 55.2 mV, intercept = -5.2 mV vs SHE.

potentials.<sup>52</sup> It was found that the potentials were within experimental error of each other ( $-132 \pm 2$  mV, respectively, vs Ag/AgCl). (These values have not been converted to SHE because junction potentials were not measured. The specific values obtained are of less importance to this study than the equivalence of the two potentials, within experimental error, when measured under the same conditions.)

## Discussion

**Structural Analysis. (a) Influence of Hemin Substituents on Electronic/Molecular Structure.** Ferricytochrome *b*<sub>5</sub> exhibits hyperfine shifts which are overwhelmingly contact for the heme pyrrole substituents and necessarily dipolar for the noncoordinated amino acid residues.<sup>40,53,54</sup> The contact shift pattern reflects the

**Table II.** The Reduction Potential of Cytochrome *b*<sub>5</sub> Reconstituted with Chemically Modified Hemins (0.13 M Phosphate Buffer, pH 7.0, *T* = 28 °C)

hemin symbol	common name	<i>E</i> <sup>o</sup> , mV (vs SHE)	slope
1B	protohemin IX <sup>a,b</sup>	$-1.9 \pm 1.6^c$	
1C	deuterohemin <sup>b</sup>	$-51.8 \pm 4.3$	$56.5 \pm 0.3^c$
1D	pemtohemin	$-7.6 \pm 2.7$	$60.1 \pm 0.9$
1E	isopemtohemin	$-38.0 \pm 1.7$	$61.9 \pm 0.5$
1F	protohemin III	$-5.2 \pm 0.0$	$55.2 \pm 0$
1G	protohemin XIII	$-1.0 \pm 2.0$	$58.8 \pm 2.6$
1H	2,4-dimethyldeuterohemin	$-83.3 \pm 1.8$	$63.7 \pm 1.2$
1J		$-93.0 \pm 0.6$	$55.9 \pm 2.3$
1K		$-84.6 \pm 2.3$	$50.4 \pm 2.7$
1L		$-58.4 \pm 5.6$	$60.3 \pm 0.9$
1M		$-76.7 \pm 1.4$	$60.3 \pm 2.1$
1N		$-75.8 \pm 3.0$	$56.2 \pm 3.2$
1P		$-67.8 \pm 3.6$	$59.1 \pm 0.9$

<sup>a</sup> Data for native equilibrium (8:1) disordered protein taken from ref 32. <sup>b</sup> The reduction potentials for protein with hemins 1B, 1C have been reported in refs 17 and 28. Our data are consistent with the reported values,<sup>17,28</sup> considering the slightly different experimental conditions. <sup>c</sup> Mean values and range for two separate trials.

orientation of the axial His, while the dipolar shifts reflect the orientation of the magnetic axes and magnetic anisotropies of the heme iron;<sup>53</sup> even small changes in the heme pocket structure can perturb the electronic/magnetic properties. Comparison of the <sup>1</sup>H NMR shifts for the ferricytochrome complexes of the hemins of interest in this study reveals<sup>30,37,39,40</sup> essentially *invariant* hemin contact shift and amino acid dipolar shift patterns. It can be concluded, therefore, that the protein folding is largely unperturbed upon modifying the heme peripheral vinyl or propionate groups and that significant changes in reduction potential reflect primarily (localized) electronic influences on the relative stabilities of the oxidized and/or reduced states.

The majority of the reconstituted proteins exhibit a single, unique orientation of the heme in the binding pocket. For the

(52) Soret  $\lambda_{\max}$ (pempto- and isopemtohemin(NMeIm)<sub>2</sub><sup>+</sup>) = 406 nm;  $\lambda_{\max}$ (pemtoheme(NMeIm)<sub>2</sub>) = 418 nm;  $\lambda_{\max}$ (isopemtoheme(NMeIm)<sub>2</sub>) = 416 nm.

(53) La Mar, G. N. In *Biological Application of Magnetic Resonance*; Shulman, R. G., Ed.; Academic Press: New York, 1979; pp 305-343.

(54) Keller, R. M.; Wüthrich, K. *Biochim. Biophys. Acta* **1972**, *285*, 326-336.

hemins **1F–1K**, the structural homogeneity is guaranteed by the 2-fold symmetry axis through the  $\alpha,\gamma$ -meso positions. In the case of hemins **1L**, **1M**, and **1N**, a unique orientation (>98%) is provided by the extremely high and specific affinity for the *g*-position propionate link to the protein matrix. However, while isopemphthohemin (**1E**) and deuterohemin (**1C**) exhibit a single orientation, native protohemin (**1B**) and pemphthohemin (**1D**) exhibit<sup>30,37,39,56</sup> ~10 and ~20% populations, respectively, with the non-methyl substituents at positions *a* and *c* rather than *b* and *d* (see A in Figure 1). Such a difference in orientation of heme can by itself lead to a difference in reduction potential due to altered protein contacts. However, the inability to experimentally differentiate the potential for heme **1E** in the two orientations due to rapid reorientation<sup>30</sup> dictates we compare only the average values for equilibrium-disordered hemins. Since the alternate heme orientations can lead to 30-mV differences<sup>32</sup> in  $E^0$ , and the "wrong" orientation in the hemins of interest is populated<sup>30,37</sup> up to 20%, we restrict interpretation of reduction potentials among the various cytochrome complexes reconstituted with the hemins only if the differences are larger than ~10 mV.

**(b) Structural Comparison to Rat Ferricytochrome  $b_5$ .** The <sup>1</sup>H NMR traces, and hyperfine shift pattern reflected therein, for the hemins **1K**, **1M**, and **1N** in bovine ferricytochrome  $b_5$  are essentially the same as found previously for the rat protein.<sup>36</sup> In both proteins there is a strong preference<sup>36</sup> at position *g* for a single propionate; hence, the only non-native equilibrium positions that are observed to be occupied by a propionate are at *e* and *h* in Figure 1A. The highly similar contact shift patterns and molecular structures of rat and bovine ferricytochromes reconstituted with the other hemins illustrated in Figure 1, as well as many others, have been noted previously.<sup>36,37</sup> The minor sequence differences<sup>21,22</sup> in the binding pocket between the two genetic variants appear to manifest themselves primarily in a clearly observable difference in the relative stabilities of the two heme orientations, as discussed in detail previously.<sup>37</sup> The one heme which resulted in a systematic difference in the contact shift pattern between rat and bovine ferricytochrome  $b_5$  is heme **1N**,<sup>34</sup> which possesses both propionates on the same pyrrole. We had earlier shown<sup>36</sup> for heme **1N** in rat ferricytochrome  $b_5$  that the anomalous shift pattern and its unusual response to both temperature and pH reflect a dynamic equilibrium between two structures which differed in the alternate salt link to the protein matrix through either the *g*-position or *h*-position propionate. The contact shift pattern for the heme N substituted bovine protein more closely resembles that observed for the remainder of the hemins which possess the *g*-propionate link to the protein.

**Reduction Potentials. (a) Vinyl Influences.** The reduction potentials of native bovine cytochrome  $b_5$  (heme **1B**) and its complex reconstituted with deuterohemin (**1C**) have been reported earlier.<sup>17,28,32</sup> Our results are consistent with these values despite some differences in ionic strength and nature of the salt. It has been proposed that the major factor affecting the reduction potential of these two proteins is the difference in porphyrin basicity, as influenced by the 2,4-substituents (2,4-vinyls,  $E^0 \sim -2$  mV; 2,4-H,  $E^0 \sim -52$  mV). We add to this series the data on heme **1H** (2,4-dimethyldeuterohemin) which leads to further stabilization of the ferric state with  $E^0 \sim -83$  mV.

While the difference between the native protohemin (heme **1B**) and deuterohemin (heme **1C**) cytochrome  $b_5$  reduction potentials must arise from the electron withdrawing influences of the vinyls,<sup>55,56</sup> the data on protein complexes of pemphthohemin (**1D**) and isopemphthohemin (**1E**) clearly show that the two vinyls differentially influence the redox potential. Although these two hemins exhibit essentially identical reduction potential outside the protein in DMF solution (see above), in the cytochrome  $b_5$  matrix heme **1D** has a reduction potential (ca. -8 mV) closer to that of native protein (ca. -2 mV), while heme **1E** exhibits a reduction

potential (ca. -38 mV) closer to that of deuterohemin (ca. -52 mV). Hence, we conclude that the 4-vinyl group accounts for the dominant electron withdrawing influence on the porphyrin skeleton of the native protein, with the 2-vinyl group providing a more minor effect.

Mauk et al. have proposed<sup>17</sup> that the vinyl orientations can influence redox potential. The modulation of the electron withdrawing property was proposed<sup>17,29</sup> to arise through the variable degree of coplanarity of vinyls and heme  $\pi$  systems, with the maximum (minimum) effect occurring when the two systems are coplanar (perpendicular). We had shown<sup>40</sup> previously that the NOEs from vinyl to adjacent meso-H and methyls in native ferricytochrome  $b_5$  reflect an in-plane and cis-oriented 4-vinyl group. The original X-ray crystal structure proposed<sup>17,22</sup> that both vinyls are oriented close to in-plane, but this refinement was based on the wrong orientation of the heme.<sup>23</sup> For the 2-vinyl group, we have observed<sup>40</sup> a NOE pattern from the vinyl to adjacent meso-H and methyl that was interpreted on the basis of a largely in-plane vinyl but with relatively unrestricted oscillatory mobility. These NOE constraints, however, are similarly consistent with a vinyl group oriented largely perpendicular to the heme. Hence the NOE data reported<sup>40</sup> previously are consistent with a sterically clamped, largely in-plane 4-vinyl group (maximal electron withdrawing), and a mobile, largely out-of-plane 2-vinyl group (minimal electron withdrawing). The present results on bovine cytochrome  $b_5$  reconstituted with pemphthohemin (**1D**) and isopemphthohemin (**1E**) provide dramatic evidence not only for the effect of vinyl orientation on reduction potential but also that it is operative differentially for the two vinyls.

The reduction potentials for the two symmetric protohemin type isomers, protohemin III (**1F**) and protohemin XIII (**1G**), both exhibit  $E^0$  close to that of the native protein ( $E^0 \sim -5$  and  $-1$  mV, respectively). This would indicate that the *a*-position or 1-vinyl and *b*-position or 2-vinyl group, as well as the *c*-position or 3-vinyl and *d*-position or 4-vinyl group, must have, pairwise, similar out-of-plane and in-plane orientations, respectively. The NOE data involving the *a*-position vinyl of protohemin XIII (Figure 4) are virtually identical with those reported for the *b*-position in the native protein. Similarly, the vinyl NOE pattern for the *c*-position vinyl of protohemin III (Figure 5) is the same as found for the *d*-position vinyl in the native protein. Hence the protein-heme contacts over the pyrrole with positions *c* and *d* are much more sterically restricting than for the pyrrole with positions *a* and *b* in Figure 1A. A similar conclusion<sup>37</sup> had been reported previously based on the heme orientational preferences for a series of hemins variably substituted at positions *a–d*, with the largest steric constraints shown to arise from the interaction of the heme with the hydrophobic cluster composed of Leu 23,25.

**(b) Propionate Influences.** Previous studies on native<sup>12</sup> and mutated<sup>20</sup> bovine cytochrome  $b_5$  and their complexes with diesterified heme revealed 64 and 67 mV, respectively, more positive  $E^0$  upon esterification, which was interpreted as supporting the proposed charge stabilization of the ferric state by a heme propionate. This role was attributed<sup>17,18</sup> to the *g*-position propionate which is oriented so as to bring the carboxylate group close to the iron(III); in the reduced protein this interaction is negated by binding an alkali metal ion to the 7-propionate.<sup>21</sup> The present data on hemins with perturbed carboxylate side chains show that such modifications lead to significant changes in reduction potential but do not support an important role to the structurally distinct *g*-position propionate.  $E^0$  for the cytochrome  $b_5$  complex of heme **1H** and heme **1L** are -83 and -58 mV, respectively, for a difference of 25 mV more positive  $E^0$  upon removing only the *f*-position, solvent extended propionate (the *g*-position propionate is conserved). Since the electronic inductive influence of a methyl and propionate are essentially identical,<sup>58</sup> the increase in  $E^0$  cannot be ascribed to inductive effects. Since removal of both propionate charges by esterification raises the potential by 64–67 mV,<sup>12,20</sup> this leaves only a 39 to 42 mV contribution to the

(55) While a vinyl group could, in principle, act as either an electron withdrawing or donating substituent,<sup>56,57</sup> the observed effect is consistent with the vinyls in this system being electron withdrawing.

(56) Charton, M. *Prog. Phys. Org. Chem.* **1988**, *16*, 287–315.

(57) Bernasconi, C. F. Personal communication.

(58) La Mar, G. N.; Viscio, D. B.; Smith, K. M.; Caughey, W. S.; Smith, M. L. *J. Am. Chem. Soc.* **1978**, *100*, 8085–8092.

increased  $E^0$  from the g-position propionate involved in the hydrogen bonding to Ser 64. Therefore, the g-position propionate is only slightly more effective (by  $\sim 15$  mV) than the f-position propionate in raising  $E^0$ , and this argues directly against the uniquely oriented 7-propionate of native cytochrome  $b_5$  as providing an important stabilizing interaction for the oxidized protein.

The above conclusions are further supported by the effect on reduction potential for the symmetric hemins with variable length carboxylate side chains. Shortening the carboxylate side chains to acetates (hemin **1K**) should prevent the g-position group from being oriented to bring the carboxylate group as close to the iron as with propionate side chains with hemin **1H**. The reduction potentials for these two protein complexes, however, are indistinguishable (ca.  $-83$  and ca.  $-85$  mV, respectively). When the carboxylate chains are lengthened to butyrates (hemin **1J**), the 7-carboxyl side chain could get closer to the iron than a propionate (hemin **1H**). Although the reduction potential is more negative (ca.  $-10$  mV) for hemin **1J** (ca.  $-93$  mV) than **1H** (ca.  $-83$  mV), consistent with some minor stabilization for the ferric state, the difference is marginal and not significantly outside the experimental uncertainties.

Moving the f-position propionate to position e (hemin **1M**;  $E^0 \sim -77$  mV) or position h (hemin **1N**,  $E^0 \sim -76$  mV) results in

only very minor changes in reduction potential relative to that for the reference protein (hemin **1H**,  $E^0 \sim -83$  mV). Hence the exact position of a propionate, at least among those that can be accommodated by the folded protein, does not appear to be important in determining the reduction potential. However, that the influence of propionates is not simply additive is illustrated for the tripropionate hemin **1P** ( $E^0 \sim -68$  mV), for which the reduction potential does not become more negative by  $\sim 25$  mV, as might be expected on the basis of the trend for hemins **1L**  $\rightarrow$  **1H**, **1M**  $\rightarrow$  **1N**, but in fact becomes more positive than for a dipropionate hemin. The ineffectiveness of the third propionate side chain in altering  $E^0$  for the cytochrome  $b_5$  complex of hemin **1L** may be due to the fact that the e-position propionate is not ionized.

**Acknowledgment.** This research was supported by grants from the National Science Foundation (DMB-88-03611 (G.N.L.)) and the National Institutes of Health (HL-22252 (K.M.S.) and DK-31038 (F.A.W.)).

**Supplementary Material Available:** A figure illustrating 1D NOEs for the ferricytochrome  $b_5$  complex of hemin **1N** (1 page). Ordering information is given on any current masthead page.

## Allosteric Regulation of Conformational Enantiomerism. Bilirubin

Gisbert Puzicha, Yu-Ming Pu, and David A. Lightner\*

Contribution from the Department of Chemistry, University of Nevada, Reno, Nevada 89557-0020. Received September 21, 1990

**Abstract:** (4Z,15Z)-Bilirubin IX $\alpha$ , the cytotoxic yellow tetrapyrrole pigment of jaundice, readily adopts either of two interconverting, enantiomeric conformations, which are stabilized through complementary intramolecular hydrogen bonding between the pyrrole and lactam N—H and C=O residues of one dipyrinone moiety and the CO<sub>2</sub>H group of propionic acid side chains on the second dipyrinone. One conformational enantiomer can be destabilized relative to the other through allosteric action by judicious placement of methyl groups in the propionic acid side chains. Thus, insertion of a methyl group at the *pro-R* site on the  $\alpha$ -carbon of the propionic acid destabilizes the *M*-chirality intramolecularly hydrogen-bonded conformational enantiomer by introducing a severe nonbonded CH<sub>3</sub>CH<sub>3</sub> steric interaction with a pyrrole methyl substituent. In contrast, introduction of a methyl group at the *pro-S* site destabilizes the *P*-chirality enantiomer. When resolved into enantiomers, the corresponding  $\alpha$ -methylated derivatives of a symmetric bilirubin analogue, mesobilirubin XIII $\alpha$ , gave intense, bisignate circular dichroism Cotton effects ( $\Delta\epsilon_{436}^{\max} = \pm 246$ ,  $\Delta\epsilon_{392}^{\max} = \mp 135$ ) for the long-wavelength exciton transition near 433 nm ( $\epsilon_{433}^{\max} = 56\,000$ ) measured in chloroform and  $\Delta\epsilon_{425}^{\max} = \pm 121$ ,  $\Delta\epsilon_{379}^{\max} = \mp 87$  in pH 7.4 phosphate buffer ( $\epsilon_{418}^{\max} = 46\,000$ ). Thus, for the first time a bilirubin has been separated into its conformational enantiomers by a forced resolution originating from internal steric effects.

Normal human metabolism produces and eliminates some 300 mg per individual per day (representing the breakdown of approximately  $10^{11}$  red blood cells/day) of the yellow pigment of jaundice, bilirubin, which is intrinsically unexcretable and cytotoxic.<sup>1,2</sup> What limits the facile excretable of bilirubin is its poor solubility in water,<sup>3</sup> its high lipid/water partition coefficient<sup>1</sup> and its proclivity to form association complexes with serum albumin and other proteins<sup>1-4</sup>—three interrelated properties that dominate the transport and metabolism of bilirubin in vivo.<sup>2,5</sup> However, the interesting biologic and unusual solubility properties

of the pigment do not correlate well with conventional linear and porphyrin-like structural representations (Figure 1). If bilirubin adopted such conformations, which are sterically disfavored as seen from CPK space-filled molecular models, it would be predictably polar and not lipophilic.

A unique conformation, which appears to play a central role in explaining many of the properties of bilirubin, is formed by rotating the two dipyrinone groups about the connecting CH<sub>2</sub> linkage so as to generate a bent or folded shape (Figure 2) in the tetrapyrrole molecule. This is the shape of bilirubin found in X-ray crystal structures of the pigment<sup>6a,b</sup> and analogues in which the vinyl groups are replaced by ethyl (mesobilirubin).<sup>6c</sup> In this conformation, which is computed to lie at or near the global energy

(1) McDonagh, A. F.; Lightner, D. A. *Pediatrics* **1985**, *75*, 443-455.

(2) For leading references, see: Ostrow, J. D., Ed. *Bile Pigments and Jaundice*; Marcel-Dekker: New York, 1986.

(3)  $K_{sp}$  for bilirubin in water at 37 °C estimated to be  $\sim 3 \times 10^{-15}$  M; Brodersen, R. in ref 2, p 158.

(4) McDonagh, A. F. In *The Porphyrins*; Dolphin, D., Ed.; Academic Press: New York, 1979; Vol. 6, pp 293-491.

(5) For leading references, see: Heirwegh, K. P. M., Brown, S. B., Eds. *Bilirubin*; CRC Press: Boca Raton, FL, 1982; Vols 1 and 2.

(6) (a) Bonnett, R.; Davies, J. E.; Hursthouse, M. B.; Sheldrick, G. M. *Proc. R. Soc. London, B* **1978**, *202*, 249-268. (b) LeBas, G.; Allegret, A.; Manguen, Y.; DeRango, C.; Bailly, M. *Acta Crystallogr., Sect. B* **1980**, *B36*, 3007-3011. (c) Becker, W.; Sheldrick, W. S. *Acta Crystallogr., Sect. B* **1978**, *B34*, 1298-1304.